

Field Trial Results for a Coordinated Multi-Point (CoMP) Uplink in Cellular Systems

Michael Grieger, Patrick Marsch, Zhijun Rong and Gerhard Fettweis
Technische Universität Dresden, Vodafone Chair Mobile Communications Systems
Email: {michael.grieger, marsch, zhijun.rong, fettweis}@ifn.et.tu-dresden.de

Abstract—Theoretical research on coordinated multi-point (CoMP) in the cellular uplink claims large improvements in spectral efficiency and fairness. However, the real-world implementation of CoMP is linked with major challenges such as multi-cell synchronization and multi-cell channel estimation, which have to be addressed to make sure that CoMP finds its way into next generation cellular systems (e.g. LTE-Advanced). In this paper, we provide a proof-of-concept that uplink CoMP concepts do in fact yield significant spectral efficiency gains in an outdoor deployment of two cooperating base stations and two terminals. We further show that the performance gains of CoMP in various interference scenarios corresponds quite well with predictions from theory.

I. INTRODUCTION

The increasing demand for higher transmission rates in cellular mobile communication systems requires that spectrum is used as efficiently as possible, which requires that radio resources are reused in each cell. The occurring inter-cell interference, however, is not sufficiently addressed in LTE Release 8 [1], which leads to a strong performance degradation of cell-edge users.

It is well-known that an information exchange among base stations for the purpose of coordinated multi-point (CoMP) detection or transmission allows exploiting inter-cell signal propagation rather than treating it as a curse, yielding large spectral efficiency and fairness gains [2], [3]. However, the benefits of CoMP come at a high cost in terms of complexity and additional infrastructure required. Some important technical challenges are the synchronization in time and frequency of all cooperating entities [4], the estimation of the CoMP channel [5], as well as backhaul-efficient multi-cell signal processing [6], [7].

The focus of the EASY-C project [8] is to assess the potential gains of CoMP vs. the efforts required to achieve these under real-world conditions. In this paper, we present measurement results for an uplink setup where two terminals (UEs) are jointly detected by two cooperating base stations (BSs). We vary the location of the UEs to create symmetric and asymmetric scenarios, and compare the results to gain predictions from information theory.

The paper is organized as follows. In Section II, we describe the measurement setup. The signal processing architecture is addressed in Section III. Information theoretic basics are reviewed in Section IV. In Section V, we present and discuss measurement results. The paper is concluded in Section VI.

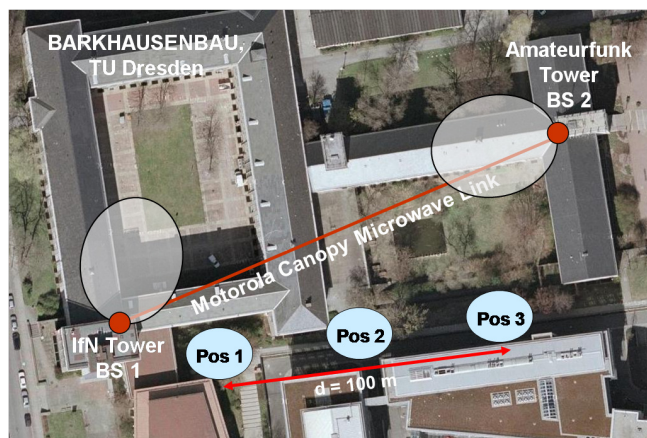


Fig. 1: Measurement setup (by courtesy of Google maps!)

Carrier frequency	2.53 GHz
System bandwidth	10 MHz
Resource blocks (PRBs)	30
No. of sub-carriers per PRB	12
Transmit Power	-5 dBm
Quantization resolution	12 bit per real dimension

TABLE I: Transmission parameters

II. MEASUREMENT SETUP

The measurement setup is depicted in Figure 1. We can see shows the location of two BSs deployed on the rooftop of a building in Dresden, which are connected through a microwave link. The BSs are synchronized through GPS fed reference normals that ensure a fine synchronization on a sample basis and each one is equipped with a cross-polarized dual antenna of type KATHREIN 80010541. The measurements are performed in a way such that the UEs are allocated to the same fixed time and frequency resources and transmit continuously using a sequence of different modulation and coding schemes (MCSs), as listed in Table I, employing one transmit antenna each. In contrast to LTE Release 8, the UEs use orthogonal frequency division multiplex (OFDM), since this strongly simplifies multi-user equalization as compared to single-carrier FDMA. In our particular prototype setup, the received signals are quantized and recorded for later offline evaluation. An overview of the measurement concept is depicted in Figure 2, and various other relevant transmission parameters are listed in Table I.

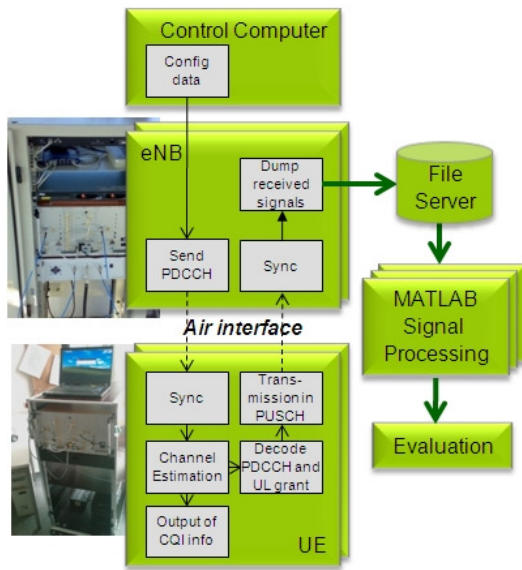


Fig. 2: Overview of the measurement concept.

III. SIGNAL PROCESSING ARCHITECTURE

Neglecting residual synchronization errors and assuming the channel has a coherence bandwidth significantly larger than the sub-carrier spacing of $\Delta F = 15$ kHz, the transmission of each symbol on a single sub-carrier of the OFDM system in frequency domain can be stated as

$$\begin{aligned} \mathbf{y}_1 &= \mathbf{h}_{1,1}x_1 + \mathbf{h}_{1,2}x_2 + \mathbf{n}_1, \\ \mathbf{y}_2 &= \mathbf{h}_{2,1}x_1 + \mathbf{h}_{2,2}x_2 + \mathbf{n}_2, \end{aligned} \quad (1)$$

where $\mathbf{y}_m \in \mathbb{C}^{[N_{\text{bs}} \times 1]}$ denotes a vector of received by N_{bs} antennas of BS m , $\mathbf{h}_{m,n} \in \mathbb{C}^{[N_{\text{bs}} \times 1]}$ denotes the channel gain matrix from UE n to BS m , $x_n \in \mathbb{C}$ is a symbol transmitted by UE n , and $\mathbf{n}_m \in \mathbb{C}^{[N_{\text{bs}} \times 1]}$ denotes additive, uncorrelated noise.

The complete receiver signal processing chain is depicted in Figure 3. In the following, we will address its elements in more detail.

A. Synchronization

As explained in Section II, the carrier frequency of the BSs is synchronized by using GPS fed reference normals, which is accurate enough for remaining errors to be neglected [9]. The frequency offset of the UEs is precompensated using reference signals that are transmitted over the downlink. Compared to the sub-carrier spacing, the remaining offset of less than 200 Hz is small enough to disregard co-channel interference. The remaining common phase error (CPE) is taken into account by an appropriate interpolation of the channel estimates, as will be explained in the next section. The frame and symbol synchronization is based on the autocorrelation properties of the OFDM time domain signal. For more details, we refer to [10].

B. Channel Estimation

For channel estimation, we choose a pilot based approach. The pilot positions are the same as those standardized for LTE

Rel. 8 [1], i.e. within each uplink transmit time interval (TTI) consisting of 14 OFDM symbols, pilots are mapped on all sub-carriers of the 4th and 11th OFDM symbols. Provided that the channel coefficient of two neighboring sub-carriers are equal, interference between pilot symbols of different UEs is avoided by a code orthogonal design using Frank-Zadoff-Chu sequences. Accordingly, each user is identified by a user-specific phase rotation $\exp(j\pi nk)$ multiplied with the baseline pilot sequences, where k and n are the sub-carrier index and the user index, respectively. At the receiver side, the multi-user channel estimation can be performed by a simple Hadamard approach as is well known from MIMO channel estimation theory [11]. Due to the spreading factor of two, the channel is estimated for every second sub-carrier in the frequency domain. In order to estimate the channel for all other sub-carriers, time and frequency interpolation are carried out separately. Due to synchronization and common phase errors between UEs and BSs, resulting in a linear phase drift over time and frequency, the channel coefficients are interpolated with respect to amplitude and phase separately. The estimated channel links, which inherently contain transmit power are determined based on the assumption of unit transmit power per UE, are denoted by $\hat{\mathbf{h}}_{m,n}$.

C. Noise Covariance Estimation

The estimation of the noise covariance is based on the channel estimates $\hat{\mathbf{h}}_{m,n}$. Because orthogonal pilot sequences are used, we are able to estimate the noise covariance independent from interference of the other UE. The particular estimation procedure relies on the assumption that the channel of two neighboring sub-carriers is equal and that the noise on different sub-carriers is uncorrelated. Based on this assumption, we can exploit the autocorrelation properties of $\hat{\mathbf{h}}_{m,n}$ to separate its noise and signal components. Subsequently, the power of these components is estimated. For a robust estimation, the determined values are averaged over both pilot sequences of each TTI and over the receive antennas. Using this approach, one noise variance $\hat{\sigma}_m^2$ can be determined per BS.

D. Channel Equalization

For symbol detection, we examine four different schemes all based on linear unbiased MMSE equalization.

- 1) Both UEs are detected by a different BS. The UE - BS assignment may be swapped.
- 2) Both UEs are detected by BS 1
- 3) Both UEs are detected by BS 2
- 4) Both UEs are jointly detected by one of the BSs, assuming that quantized frequency-domain receive signals are exchanged over the backhaul with 24 bits per complex symbol per sub-carrier.

For all non-cooperative options (1 - 3), the MMSE equalization filter for the detection of one particular receive symbol of UE n at BS m is given by

$$\mathbf{G}_{\text{biased}}^{[m,n]} = \hat{\mathbf{h}}_{m,n}^H \left(\hat{\mathbf{h}}_{m,n} \hat{\mathbf{h}}_{m,n}^H + \hat{\mathbf{h}}_{m,\bar{n}} \hat{\mathbf{h}}_{m,\bar{n}}^H + \hat{\sigma}_m^2 \mathbf{I} \right)^{-1}, \quad (2)$$

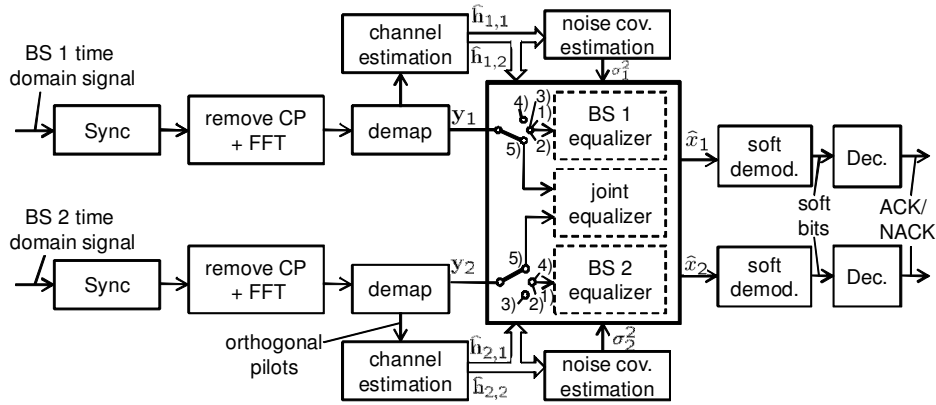


Fig. 3: Receiver chain

where \bar{n} is the index of the interfering UE. The MMSE filter for joint detection is

$$\mathbf{G}_{\text{biased}} = \hat{\mathbf{H}}^H \left(\hat{\mathbf{H}}\hat{\mathbf{H}}^H + \hat{\mathbf{\Phi}} \right)^{-1}, \quad (3)$$

where $\hat{\mathbf{H}} = \begin{bmatrix} \hat{\mathbf{h}}_{1,1} & \hat{\mathbf{h}}_{1,2} \\ \hat{\mathbf{h}}_{2,1} & \hat{\mathbf{h}}_{2,2} \end{bmatrix}$ and $\hat{\mathbf{\Phi}} = \begin{bmatrix} \hat{\sigma}_1^2 \mathbf{I} & 0 \\ 0 & \hat{\sigma}_2^2 \mathbf{I} \end{bmatrix}$.

The output of both filters is biased which results in an increased bit error probability for higher order modulation schemes such as 16QAM. For this reason, we resort to the unbiased MMSE filter, which is given by the following expression

$$\mathbf{G} = \left(\text{diag} \left(\text{diag}^{-1} \left(\mathbf{G}_{\text{biased}} \right) \right) \right)^{-1} \mathbf{G}_{\text{biased}}, \quad (4)$$

where $\text{diag}(\cdot)$ takes a vector of size N to a diagonal matrix of size $N \times N$, and $\text{diag}(\cdot)^{-1}$ maps the diagonal elements of any square matrix of size $N \times N$ to the entries of a size N vector. Hence, if $\text{diag}(\cdot)^{-1}$ and $\text{diag}(\cdot)$ are used successively, the off diagonal elements of the resulting matrix are all zero.

Since the BSs estimate the channel towards each UE (even in the non-cooperative case) the BSs are able to reduce interference by taking it into account in the determination of the equalization filter. In LTE, this feature is referred to as interference rejection combining.

E. Soft Demodulation and Decoding

The soft demodulation is based on the equalizer output and signal-to-interference-and-noise ratios (SINRs) which are estimated according to a standard error vector magnitude approach [12]. The demodulator output is subsequently fed into the decoding chain, which, together with the used codes is basically compliant to LTE Rel. 8. The employed codes are listed in Table II. Each codeword spans one TTI in time domain and all 30 PRBs in frequency domain. The decoding success is determined by an outer CRC check, also a standard procedure.

IV. INFORMATION THEORY

Previous publications clearly show that CoMP offers high gains in terms of capacity when compared to non-cooperative communication [3]. However, actual gains achievable in real systems can be determined in field trials only. Therefore,

MCS#	Mod. scheme	Code rate	Peak rate	Bit per channel use
1	4QAM	2/3	4.54 Mbps	1.34
2	16QAM	1/2	6.91 Mbps	2.00
3	16QAM	2/3	9.29 Mbps	2.66
4	16QAM	3/4	10.6 Mbps	3.00
5	16QAM	6/7	12.3 Mbps	3.43

TABLE II: Modulation schemes and code rates used for transmission, assuming turbo codes as used in LTE Rel. 8.

comparing theoretical results with measurement results is of great interest. The information theoretic fundamentals for this comparison are recapitulated in this section. The fundamental limits for achievable transmission rates are given by Shannon's definition of channel capacity. Since our setup is constrained to linear detection strategies—in particular we do not consider interference cancellation—we are not able to achieve channel capacity. Instead, the maximum achievable rates are given by the well known Shannon type equations for the Gaussian multi-user MIMO channel with linear MMSE receivers. If the BSs do not cooperate, the achievable rates depend on the choice of the BS, detecting a particular UE. Assuming a channel realization that is flat in the frequency domain and static at least for one TTI, the rate of UE n which is detected at BS m is given by

$$R_{m,n} = \log_2 \left| 1 + \mathbf{h}_{m,n}^H \left(\mathbf{h}_{m,\bar{n}} \mathbf{h}_{m,\bar{n}}^H + \sigma_m^2 \mathbf{I} \right)^{-1} \mathbf{h}_{m,n} \right|, \quad (5)$$

In (5), the transmit power is normalized to one, which is always possible by adjusting the channel gains accordingly.

On the other hand, if both UEs are decoded jointly, the achievable rates are given by

$$R_n = \log_2 \left| 1 + \mathbf{h}_n^H \left(\mathbf{h}_{\bar{n}} \mathbf{h}_{\bar{n}}^H + \begin{bmatrix} \hat{\sigma}_1^2 \mathbf{I} & 0 \\ 0 & \hat{\sigma}_2^2 \mathbf{I} \end{bmatrix} \right)^{-1} \mathbf{h}_n \right|, \quad (6)$$

where $\mathbf{h}_n = \begin{bmatrix} \mathbf{h}_{1,n} \\ \mathbf{h}_{2,n} \end{bmatrix}$ and $\mathbf{h}_{\bar{n}} = \begin{bmatrix} \mathbf{h}_{1,\bar{n}} \\ \mathbf{h}_{2,\bar{n}} \end{bmatrix}$.

V. COMPARISON OF THEORETICAL AND MEASURED RATES

In this section, we compare the terminal rates that should be achievable according to information theory to rates actually

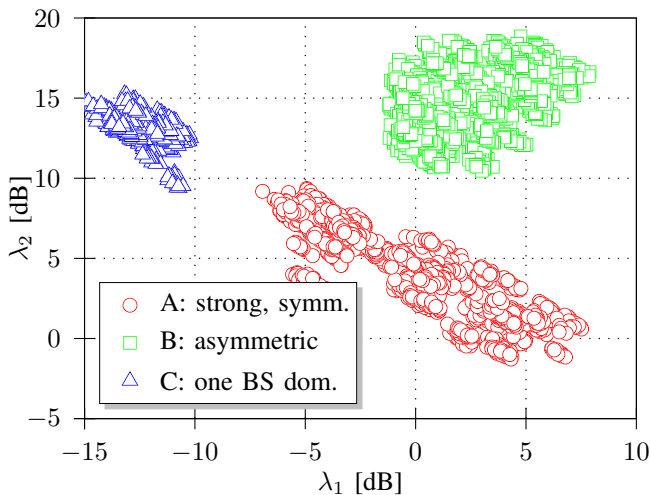


Fig. 4: Identification of interference scenarios to be discussed in this paper.

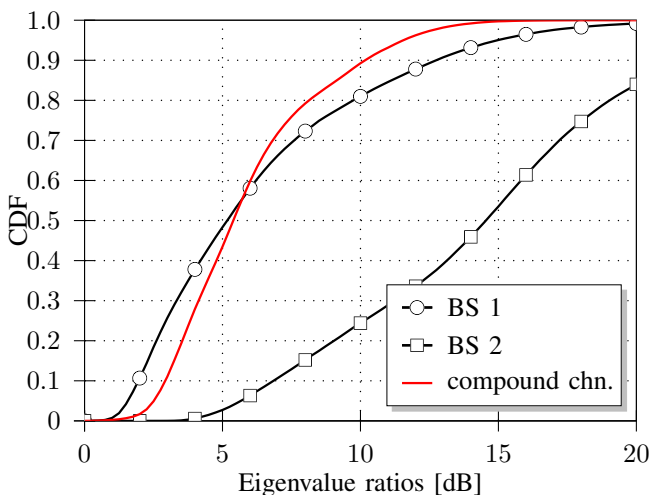


Fig. 5: Eigenvalue distribution for scenario A with $N_{bs} = 2$.

measured in the field trial described in Section II. In both cases, we observe the performance achievable if detection and decoding takes place non-cooperatively by the two BSs, or jointly. The information theoretic numbers are computed for each 12th sub-carrier and each 7th OFDM symbol according to (5) and (6), using the channel coefficients and noise levels obtained in the field trial. Here, the inherent assumption is that the estimated channel corresponds to the real channel, and that the receiver side has perfect CSIR, which clearly leads to a strong overestimation of rates. In this work, however, we are mainly interested in the *gain* of CoMP in different scenarios, where the correlation between theoretically and measured results is strong, as we will see in the sequel.

For rate expressions based on actual transmissions, we collect statistics for the 5 different MCSs stated in Table II. For each transmission of 20 TTIs, we then determine the MCS that has led to the highest overall number of successfully transmitted bits, and translate this quantity into a corresponding average number of bits per channel use. Clearly, *automatic repeat-request* (ARQ) concepts could help to improve the

reliability of transmission and hence increase achieved rates, but they would lead to a more complex field trial setup. In general, the rates based on field trial transmissions are of course much lower than those based on information theory, as the former are constrained through a very limited set of MCSs and are deteriorated due to limited block lengths, multi-cell channel estimation error, noise estimation error as well as various RF impairments.

As stated in Section II, we have performed measurements for various UE locations, yielding a variety of interference scenarios. In order to characterize these, we introduce the terms λ_1 and λ_2 that state the ratio of the average channel gain of a UE to its assigned BS over the average channel gain to the other BS, for UEs 1 and 2, respectively. A large value means that a UE has a significantly stronger link to its own BS than to the other one, a value of 0 dB corresponds to the case where the UE is placed at the cell-edge between both BSs, and a negative value (on a logarithmic scale) indicates that the UE has a stronger gain to the neighboring BS than to its own BS. For a subset of measurements, the λ values are shown in Figure 4, where we have identified three clusters of interference scenarios that will be observed separately in the sequel:

- **A:** Scenarios of strong, symmetrical interference
- **B:** Scenarios of asymmetrical interference
- **C:** Scenarios where both UEs have a dominant link to the same BS (in this case BS 2)

In Figure 6 we can see results for **scenario A**, where the left plot refers to the case of $N_{bs} = 1$ and the right one to $N_{bs} = 2$. Clearly, the gain of using joint multi-cell detection (red curves) instead of non-cooperative detection (black and blue curves) is large for $N_{bs} = 1$, as we have strong interference, and each BS cannot spatially separate the two terminals by itself. In information theory (solid curves), the gain is on the order of 150%, and for field trial transmission (dashed curves), BS cooperation can in fact strongly reduce the outage probability of both terminals. In the case of $N_{bs} = 2$, BS cooperation gains are smaller, but still correspond to about 50% in the case of field trial transmission. Without BS-cooperation, we can see that from an information theoretical point of view, it is beneficial for UE 2 to be detected and decoded by BS 1 \textcircled{A} . While this appears counter-intuitive considering that UE 2 in most cases has a stronger link to its assigned BS 2 (see Figure 4), the reason lies in the fact that the channel from both UEs to BS 1 has better spatial properties. This is illustrated in Figure 5, where the ratio of the first and second Eigenvalue (i.e. similar to the definition of the *condition number*) of the channel seen by BS 1 is as good (i.e. as *low*) as that of the compound channel. For field trial transmission, however, we can see that this BS-UE assignment is not beneficial \textcircled{B} , which is due to the fact that the comparatively weak link from UE 2 to BS 1 is subject to a strong channel estimation error, such that its beforementioned spatial properties cannot be reasonably exploited. Note that the reason why field trial transmission can achieve larger rates than predicted through

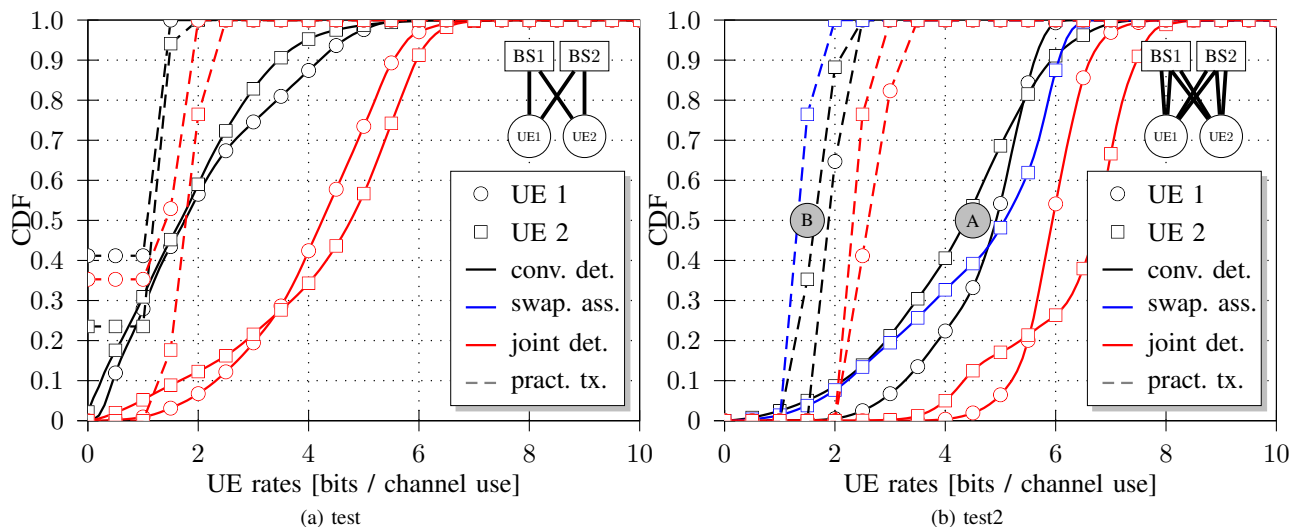


Fig. 6: Theoretical and measured UE rates for scenarios A of strong, symmetric interference.

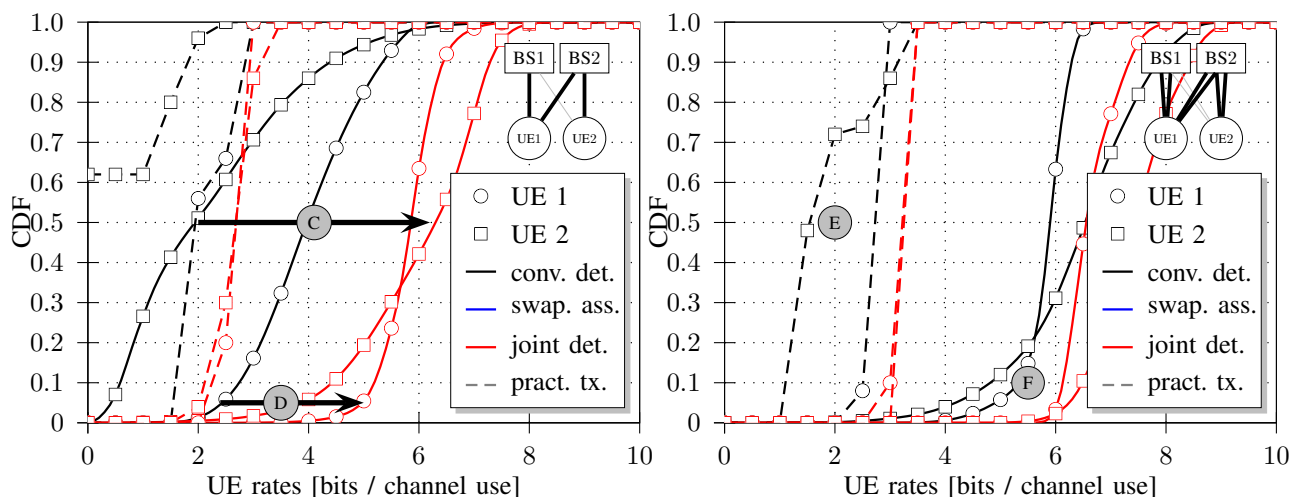


Fig. 7: Theoretical and measured UE rates for scenarios B of asymmetric interference.

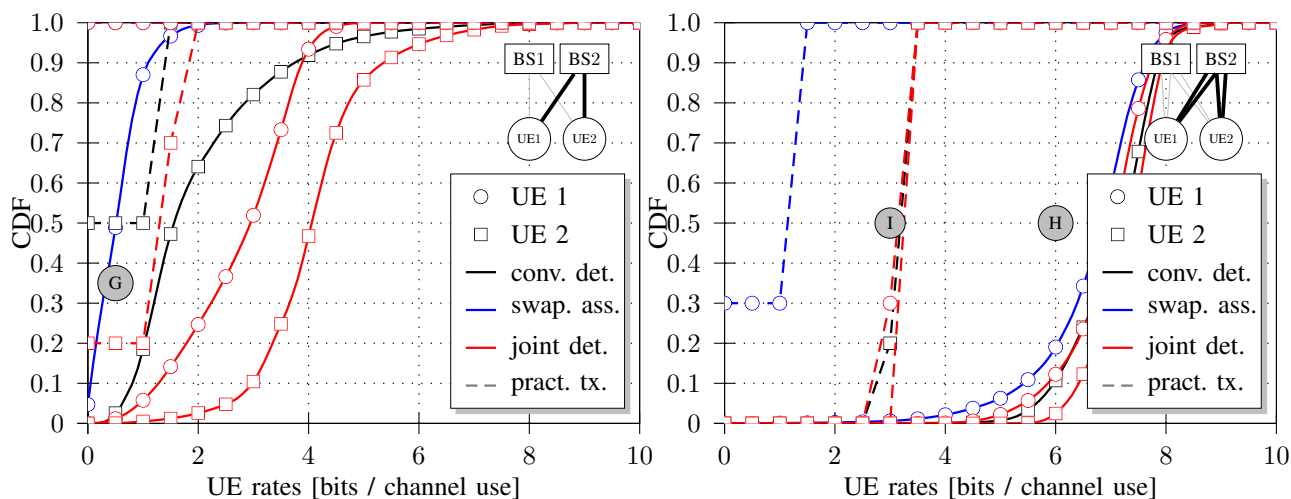


Fig. 8: Theoretical and measured UE rates for scenarios C of strong links to one BS.

information theory at the very lower end of the CDF is due to the fact that the histogram of information theoretical quantities is calculated on a per-sub-carrier basis and hence subject to a large variance, whereas the performance of implemented schemes is only available on a TTI basis, where the interleaver and decoder can alleviate the impact of some poor channel realizations.

In Figure 7, we see results for **scenario B**, where UE 1 is placed close to the cell-edge, while UE 2 has a dominant link to its assigned BS 2, creating little interference to BS 1. Clearly, UE 2 can profit most from multi-cell joint detection in this case (C), while UE 1 can be detected and decoded by its own BS 1 fairly free of interference regardless of whether BS cooperation is used or not. The latter UE, however, profits strongly from array gain and diversity (D). As expected, both aspects are less pronounced for $N_{\text{bs}} = 2$, but we can still see a significant rate improvement for UE 2 (E), while UE 1 profits from array and diversity gain (F). Please note that the reason why both UEs perform similarly in the case of field trial transmission and CoMP is that the maximum possible rate of 3.42 bits per channel use in our prototype platform has been reached.

In Figure 8, we finally observe **scenario C**, where both UEs are assigned to BS 2 (blue curve). Clearly, non-cooperative detection is subject to significant interference for $N_{\text{bs}} = 1$, and hence leads to 100% outage for both UEs under field trial transmission. Interestingly, the outage for UE 2 can be strongly decreased if multi-cell joint detection is used (G), even though the link from UE 2 to BS 1 appears to be of minor importance. UE 1, however, cannot be detected, even under cooperation. For $N_{\text{bs}} = 2$, average CoMP gains diminish from a theoretical point of view (H); only a marginal array gain is achieved. For field trial transmission, however, we can see that UE 1 strongly benefits from cooperation (I). It appears that in this scenario, the links from UE 1 to BS 2 are significantly weaker than those from UE 2 to BS 2, and the channel as seen by BS 2 is often close to singular. In theory, where we assume perfect CSI, it is still possible for BS 2 to spatially separate both terminals, while this seems to fail for field trial transmissions due to imperfect channel knowledge. Once BS cooperation is used, channel estimation can also profit from array gain and diversity, as e.g. noted in [13]. Note that field trial transmission under cooperation once again reaches the maximum possible rate of 3.42 bits per channel.

VI. CONCLUSIONS AND OUTLOOK

In this paper, we observed the gains of coordinated multi-point (CoMP) in field trial cellular scenarios of 2 base stations and 2 terminals. We saw that theoretically predicted rate gains are confirmed by those observed under field trial transmission, if we consider that the gains of the latter are typically much smaller due to the impact of imperfect channel estimation, a limited number of usable modulation and coding schemes, and various RF impairments. Furthermore, we used measurements to validate the benefit of performing a fast-fading dependent

assignment of UEs to BSs, possibly in conjunction with the option of intra-cell joint detection in the case of multiple receive antennas per base station, as it is also suggested from a theoretical point of view in [13]. In general, it seems reasonable to expect median rate gains through CoMP on the order of at least 50% and additional large diversity gains for a large set of scenarios. These effects are leading to an increase of fairness as well. It can be expected that these gains can be further increased if more advanced signal processing is applied in the future.

In future work, we plan to consider non-linear detection schemes and to observe the trade-off between achievable rates and the backhaul capacity required to achieve these. For this, we will implement and evaluate different BS-cooperation schemes as stated in [7], which mainly differ with regard to the kind of information (and inherent quantization scheme) between cooperating BSs. In the longer term, we plan to address the central question of how often in a representative middle-sized city certain interference scenarios arise for which CoMP promises substantial gains at reasonable effort, and what kind of BS cooperation schemes should ideally be used.

ACKNOWLEDGEMENT

We would like to thank the project partners for the great collaboration and the German Ministry for Education and Research (BMBF) for the funding of the project EASY-C. We further want to note that this work would not have been possible without the support from our colleagues Vincent Kotzsch, Eckhard Ohlmer, Jan Wulfes, Matthias Pötschke and Joachim Heft.

REFERENCES

- [1] W. McCoy, "Overview of 3GPP LTE Physical Layer: White Paper by Dr. Wes McCoy," *White Paper*, 2007.
- [2] P. Marsch, S. Khatkhat, and G. Fettweis, "A framework for determining realistic capacity bounds for distributed antenna systems," in *Proceedings of the IEEE Information Theory Workshop (ITW'06)*, Oct. 2006.
- [3] S. Venkatesan, "Coordinating base stations for greater uplink spectral efficiency in a cellular network," in *Proc. PIMRC*, 2007.
- [4] M. Schellmann and V. Jungnickel, "Multiple CFOs in OFDM-SDMA Uplink: Interference Analysis and Compensation," *EURASIP Journal on Wireless Communications and Networking*, vol. 2009, 2009.
- [5] L. Maniatis, T. Weber, A. Sklavos, and Y. Liu, "Pilots for joint channel estimation in multi-user OFDM mobile radio systems," in *ISSSTA*, vol. 1, 2002.
- [6] P. Marsch and G. Fettweis, "A Framework for Optimizing the Uplink Performance of Distributed Antenna Systems under a Constrained Backhaul," June 2007, pp. 975–979.
- [7] —, "On Uplink Network MIMO under a Constrained Backhaul and Imperfect Channel Knowledge," *Proc. ICC*, 2009.
- [8] R. e. a. Imer, "Multisite Field Trial for LTE and Advanced Concepts," *IEEE Communications Magazine*, vol. 47, no. 2, pp. 92–98, 2009.
- [9] V. Jungnickel, T. Wirth, M. Schellmann, T. Haustein, and W. Zirwas, "Synchronization of cooperative base stations," in *Proc. ISWCS*, 2008.
- [10] M. Morelli, C.-C. Kuo, and M.-O. Pun, "Synchronization techniques for orthogonal frequency division multiple access (ofdma): A tutorial review," *Proceedings of the IEEE*, vol. 95, no. 7, July 2007.
- [11] K.-D. Kammeyer, *Nachrichtenübertragung*, 4th ed. Stuttgart, Deutschland: B.G. Teubner, Reihe Informationstechnik, Mar 2008.
- [12] R. Shafik, S. Rahman, R. Islam, and N. Ashraf, "On the error vector magnitude as a performance metric and comparative analysis," in *Proc. ICET 2006*.
- [13] P. Marsch and G. Fettweis, *Coordinated Multi-Point under a Constrained Backhaul and Imperfect Channel Knowledge*, 2010, PhD thesis.